



HAL
open science

Ionization in a frozen Rydberg gas with attractive or repulsive potentials

Matthieu Viteau, Amodsen Chotia, Daniel Comparat, Duncan Tate, Thomas F. Gallagher, Pierre Pillet

► **To cite this version:**

Matthieu Viteau, Amodsen Chotia, Daniel Comparat, Duncan Tate, Thomas F. Gallagher, et al..
Ionization in a frozen Rydberg gas with attractive or repulsive potentials. 2008, pp.4. hal-00289203

HAL Id: hal-00289203

<https://hal.science/hal-00289203>

Submitted on 20 Jun 2008

HAL is a multi-disciplinary open access archive for the deposit and dissemination of scientific research documents, whether they are published or not. The documents may come from teaching and research institutions in France or abroad, or from public or private research centers.

L'archive ouverte pluridisciplinaire **HAL**, est destinée au dépôt et à la diffusion de documents scientifiques de niveau recherche, publiés ou non, émanant des établissements d'enseignement et de recherche français ou étrangers, des laboratoires publics ou privés.

Ionization in a frozen Rydberg gas with attractive or repulsive potentials

Matthieu Viteau¹, Amodsen Chotia¹, Daniel Comparat¹, Duncan A. Tate^{*1}, T. F. Gallagher^{†1} and Pierre Pillet¹

¹ *Laboratoire Aimé Cotton, CNRS, Univ Paris-Sud,
Bât. 505, Campus d'Orsay, 91405 Orsay, France*

^{*} *Department of Physics and Astronomy, Colby College, Waterville, Maine 04901-8858, USA*

[†] *Department of Physics, University of Virginia, Charlottesville, Virginia 22904-0714, USA*

(Dated: June 20, 2008)

We report clear evidence of the role of dipole-dipole interaction in Penning ionization of Rydberg atoms, leading to the formation of an ultracold plasma. Penning ionization of np Rydberg Cesium atoms is prevented for states with $n < 42$, which correspond to a repulsive potential, but it does not occur for n larger than 42, corresponding to an attractive potential. Blackbody radiation is mostly responsible for the background and initial ionization, although ion-Rydberg collisions and population transfer due to limited superradiance may have to be considered.

PACS numbers: 32.80.Ee; 34.20.Cf; 37.10.De

A cold Rydberg gas is a fascinating system at the boundary of atomic, solid state, and plasma physics. In a MOT, at $100 \mu\text{K}$ temperature, the atoms move less than 3% of their typical separation, 10^{-3} cm , on the $1 \mu\text{s}$ time scale of the experiments, and such a sample resembles an amorphous solid. Since Rydberg atoms have large dipole moments, scaling as the square of the principal quantum number n , dipole-dipole interactions in the frozen Rydberg gas have a significant effect, even though the atoms are far apart [1, 2, 3]. For this reason, binary dipole-dipole interactions have been proposed as the basis for quantum gates [4, 5]. Specifically, the dipole-dipole interaction between a pair of Rydberg atoms can preclude the excitation of the second atom in a sample once the first is excited, a phenomenon termed the dipole blockade. Local, or partial, blockades have been observed in many experiments, such as [6] in Van der Waals case or [7] in dipole one. In addition to binary interactions, there is evidence for many body interactions roughly analogous to the diffusion of spins in a glass [8, 9]. This phenomenon is particularly apparent in the dipole-dipole energy transfer tuned into resonance with an electric field, a process often termed the Förster Resonance Energy Transfer (FRET) reaction [10].

In addition a cold Rydberg gas can spontaneously evolve into a plasma. If there is even a very slow ionization process, cold ions are produced, and at some point their macroscopic space charge traps all subsequent electrons produced [11, 12, 13]. The trapped electrons lead to a collisional avalanche which rapidly redistributes the population initially put into a single Rydberg state. Typically two thirds of the atoms are ionized and one third are driven to lower states to provide the requisite energy [11, 14]. The origin of the initial ions is not, however, completely understood [15, 16, 17]. With a pulsed laser it is possible to excite atoms close enough to each other that they interact strongly, resulting in ionization on a 100 ns time scale, too fast to be a result of motion of the atomic nuclei [18].

With narrow bandwidth, quasi continuous wave (cw) excitation, it is not possible, due to the energy shift pro-

duced by the dipole-dipole interaction, to excite atoms which are close together, yet ionization still occurs, although on a time scale of microseconds [19]. One mechanism for this ionization is that pairs of atoms excited to attractive diatomic potential curves collide, resulting in the ionization of one of the atoms. The much more rapid conversion of cold Rb nd atoms to a plasma than ns atoms was attributed by Li *et al.* to ionizing collisions of pairs of atoms excited to attractive potentials in the nd case but not in the ns case [20]. Using a narrow bandwidth laser Vogt *et al.* showed that ions are present on attractive Cs nnp potentials [10]. A similar behaviour was noticed by Amthor *et al.* where they demonstrated that pairs of atoms excited closer together on the Rb $60d60d$ attractive potential ionized more rapidly than those farther apart. A surprising aspect of their observations is the high ionization rate for the $62s$ state in spite of the repulsive $62s62s$ potential [15].

In an effort to isolate the effect of attractive/repulsive potentials from other effects, we have examined the ionization of cold Cs np atoms excited with narrow bandwidth excitation. The interest of the Cs np states is that for $n > 42$ a pair of Cs np atoms is on an attractive potential, while for $n < 42$ the potential is repulsive. Thus by varying n from 40 to 45 we switch, at $n = 42$, from excitation to a repulsive potential to an attractive one, with all other parameters of the system changing only slowly. The results show unambiguously the difference between attractive and repulsive potentials. Perhaps as interesting, in the repulsive case we observe ionization which is nearly linear in the number of excited atoms, but at a rate that is twice that due to blackbody photoionization. Our observation of such a high ionization rate is not unique; others have made similar observations [15]. We suggest here that possible sources of high ionization rates are ionizing collisions, due to motion on attractive ion-dipole potentials and dipole-dipole potentials activated by state changes stimulated by the blackbody radiation and superradiant decay. In the sections which follow we describe the Cs system we have studied, present our experimental results, and compare them to expectations

based on 300K black body population transfer.

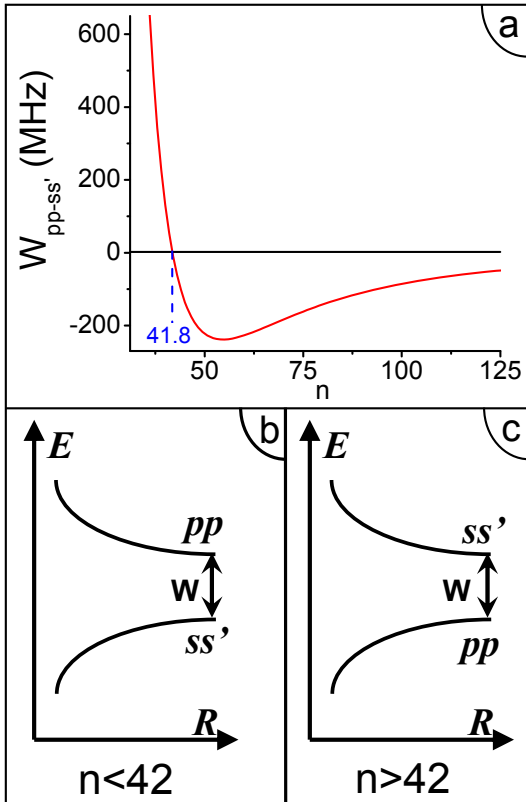


FIG. 1: (a) The energy difference (W) between the molecular pp and ss' states at $R = \infty$ for different n . (b) and (c) Schematic potential curves of pair of atoms as function of internuclear distance.

For convenience we consider the molecular state composed of a pair of Cs Rydberg atoms separated by distance R . A pair of np atoms we term the pp state, and the nearly degenerate pair of ns and $(n+1)s$ atoms we term the ss' state. The energy difference between the molecular pp and ss' states at $R = \infty$ is given by

$$W_{pp-ss'} = 2W_{np} - W_{ns} - W_{(n+1)s} \quad (1)$$

where W_{nl} is the energy of the Cs nl state. As shown by Fig.1a, $W_{pp,ss'}$ crosses zero at $n \sim 42$. For $n > 42$ the pp state lies below the ss' state, while for $n < 42$ the reverse is true. If we ignore the fine-structure and the angular distribution, the pp and ss' states are coupled by the dipole-dipole interaction $\frac{\mu\mu'}{R^3}$, where μ and μ' are the dipole matrix elements connecting the np state to the ns and $(n+1)s$ states, and at finite R the eigenstates are attractive and repulsive linear superpositions of pp and ss' . The resulting potential curves are schematically shown in Fig.1b and Fig.1c. As $R \rightarrow \infty$ the potentials are $1/R^6$ van der Waals potentials, but at small R they are $1/R^3$ dipole-dipole potentials [24]. We excite Cs atoms to the atomic $np_{3/2}$ state, or pairs of atoms to the molecular pp state. The repulsive potential is excited for $n < 42$,

the attractive potential for $n > 42$, while for $n = 42$ at high atomic density, both potentials are excited.

In the experiment Cs atoms are held in a magneto optical trap (MOT) at a temperature of $100 \mu\text{K}$ and a number density of up to $5 \times 10^{10} \text{cm}^{-3}$. The atoms are excited to the $np_{3/2}$ states via the route

$$6s_{1/2} \rightarrow 6p_{3/2} \rightarrow 7s_{1/2} \rightarrow np_{3/2} \quad (2)$$

using three cw single frequency lasers. The first laser is the 852nm trap laser, a diode laser which is typically left on continuously. Using acousto optic modulators we form the outputs of the second and third lasers into temporally overlapping pulses at an 80Hz repetition rate. The second laser is a 1470nm diode laser with a typical power of 20mW. It is focused to a beam waist of $100 \mu\text{m}$. The third laser is a Titanium:Sapphire laser operating near 830nm. It has a beam waist of $70 \mu\text{m}$, and it crosses the second laser at 67.5° , producing a $2 \times 10^{-3} \text{mm}^3$ volume of Rydberg atoms. The second and third laser pulses have a 300 ns durations. The inherent limitation of the linewidth of the final transition is imposed by the 54 ns lifetime of the Cs $7s$ state, the 1 MHz laser linewidth and the Fourier transform of the pulse duration. Subsequent to its production by the laser pulses the cold Rydberg gas is allowed to evolve for times from 450 ns to $50 \mu\text{s}$. At this time we analyze the population with a field ionization pulse which rises to 500 V/cm in 50 ns, applied using two grids 1.57 cm apart. Any ions present are ejected from the MOT at the beginning of the field ionization pulse, the Rydberg atoms are ionized, and the resulting ions are ejected later. Both sets of ions strike a microchannel plate detector, producing time resolved ion and Rydberg atom signals for initial states of $n < 80$, which are registered with two gated integrators and stored in a computer.

The data are taken by scanning the frequency of the third laser while recording the ion and atom signals, with all other parameters held fixed. In Fig.2a and Fig.2b we show typical recordings of the ion and atom signals for the $40p_{3/2}$ and $43p_{3/2}$ states respectively, for two different laser intensities. We note the asymmetrical shoulder on the red side of the line, due to the three step excitation, where direct two and three photon excitations of process (2) can occur. The time delay between the end of the laser pulse and the field ionization pulse is $10 \mu\text{s}$. At low power, i.e. at low Rydberg density, we observe in both cases a small number of ions, (7% of Rydberg atoms excited for $40p$ and 10% for $43p$). When we increase the density, for $40p$ the number of ions is still small (9%) but for $43p$ we observe, at resonance, complete ionization of the Rydberg sample, the signature of the formation of a plasma. The differences between $n = 40$ and $n = 43$ in the frequency and magnitude of the ionic signals are due to the excitation of atoms to the attractive potential in the latter case, as suggested by [20].

The maxima of spectral scans, at a fixed frequency, such as those shown in Fig.2 for a range of densities, delay times and quantum states give a more comprehensive

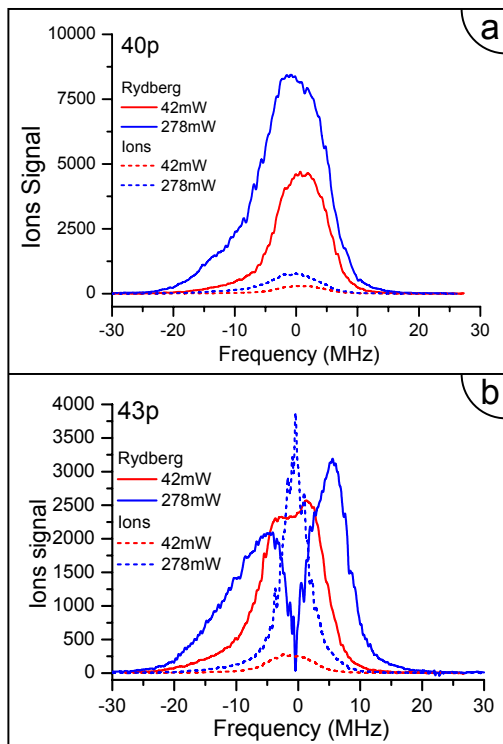


FIG. 2: Rydberg and Ion signal with two different laser intensity (42mW and 278mW) for (a) 40p state (repulsive) and (b) 43p (attractive) Data are taken after a time delay of 10 μ s, between the end of the laser pulse and the field ionization pulse.

picture. In Fig.3 we show the density of ions vs density of Rydberg atoms initially excited, for 0.45, 5, and 10 μ s delay times. The number of Rydberg atoms was varied by changing the intensity of the Ti:Sapphire laser. We note that there is a large number of ions present at a delay of 0.45 μ s, and we believe they are formed during the 300 ns laser excitation. The central features of Fig.3 are the following. With a 0.45 μ s delay the ionization yields for all n states are essentially the same, but with 5 and 10 μ s delays there is a clear difference between the $n < 42$ and $n > 42$ states. The only difference between these two cases is that the atoms are excited to a repulsive potential in the former case and an attractive one in the latter case. Two atoms excited to the 43p43p state with a separation of 5 μ m collide and ionize in 6 μ s [24]. For a Rydberg density of $25 \times 10^8 \text{ cm}^{-3}$, corresponding to 5000 Rydberg atoms in the trap, 10% of the atoms are this close together, so the difference between the $n < 42$ and $n > 42$ behaviours is evidently due to the dipole-dipole induced collisions.

For the 10 μ s delay the ion production, for $n > 42$, starts to become very nonlinear for a ion density of $2 \times 10^8 \text{ cm}^{-3}$ (~ 400 ions), which we attribute to the trapping of the electrons by the ions and the subsequent ionizing collisions of the electrons with the Rydberg atoms.

For 5 and 10 μ s delays, the 42p state is between the two sets of curves, corresponding to an excitation to both the

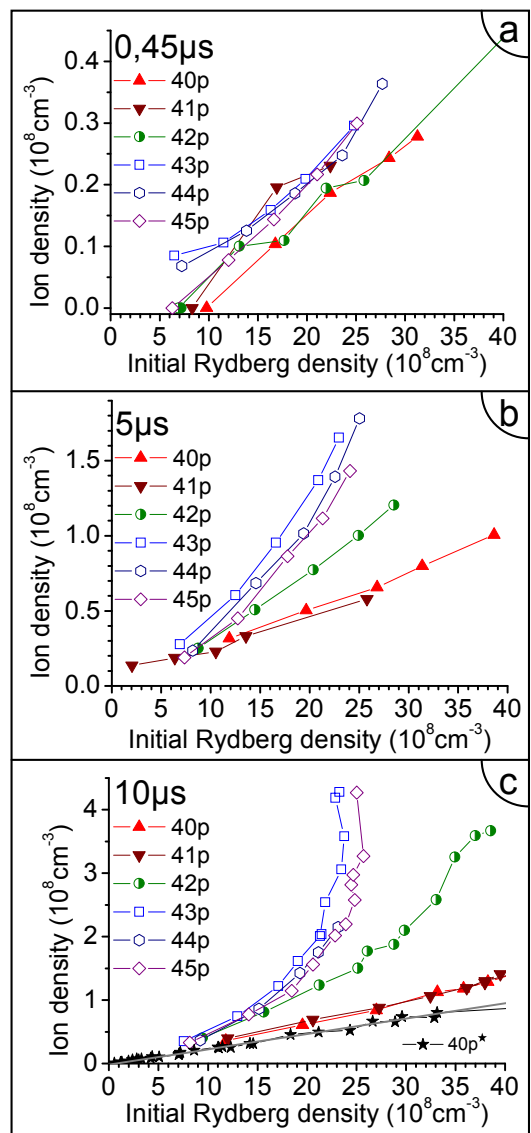


FIG. 3: Ion density as function of initial Rydberg density for different n states and three delay time (a) 0.45 (b) 5 and (c) 10 μ s. At 10 μ s the “40p*” is without 6p cold and hot atoms. Each point corresponds to the maxima of spectral scans, such as those shown in Fig.2.

repulsive and attractive potentials. While the difference between the attractive and repulsive curves of Fig.3c is understood, the source of the ionization for the $n < 42$ states is less evident.

We show two kinds of data for the repulsive case ($n < 42$). For the 40p and 41p data, 6p cold and hot atoms are present due to the trap lasers. For the data labelled “40p*” the 6s – 6p excitation is turned off at the same time as the second and third lasers are turned off, so there are no 6p atoms with which to interact. In the case of the 40p state with no 6p atoms, we observe an apparently density independent ionization rate of 2400 s^{-1} . This linear rate also appears to be present in the $n > 42$

states at low density. The calculated blackbody photoionization rate is 1200 s^{-1} [20, 21]. The observed rate is twice the calculated rate. Our observations are not unique in this regard [15]. The ionization rates for excitation to repulsive curves are generally higher than the calculated blackbody photoionization rates, and we now consider possible causes of this ionization.

One possibility is the black-body transfer of population from the np states to the nearby ns and nd states, producing $ns-np$ and $nd-np$ pairs, with a rate $\sim 10\,000 \text{ s}^{-1}$. Roughly half the pairs will be on attractive $1/R^3$ potentials and half on the repulsive potentials. Only 5% of those on attractive potentials can collisionally ionize on a $10 \mu\text{s}$ time scale, corresponding to a rate of ions formation around 250 s^{-1} , which is not fast enough to explain our observations. This rate could be, for short time scales, increased by superadiance [16, 22]. In this connection we note that, for some conditions (medium density), the Cs $40p$ state could exhibit a rapid initial decay, with a $\sim 10 \mu\text{s}$ decay time, far faster than the 300 K $40p$ lifetime of $47 \mu\text{s}$. But in most of the conditions of this article the presence of the dipolar and ionic dephasing would probably limit this effect.

We suggest here a new contribution to the large ionization rates in the case of the repulsive potentials based on the effect of cold ions, which may attract the nearest Rydberg atom by the ion-dipole interaction. The process could be the following: one ion and one Rydberg could collide to produce a translationally cold Cs_2^+ molecule, which in turn attracts another Rydberg atom, a process likely to result in two ions. However, the ions are hot, and the process terminates, so this could increase the

ionization rate up to 1000 s^{-1} rate. Taken together the above mechanisms are probably responsible for the observed ionization rates for the $n < 42$ states. We note, though, that the scenarios outlined above should lead to a nonlinear ionization rate for short times or low densities, which is not apparent in our data, although the fact that the sample of atoms does not have a uniform density may mask such features. The notion of collisions due to ion-Rydberg dipole attractive potentials assumes that the polarizability, of the Rydberg atom, is greater than zero, that is the Stark shift is to lower energy when the electric field is increased. This requirement is met for the Cs $40p$ and Rb $40s$ states, but not for the Cs $39d$ state, and it may be why the ionization rate $\sim 1000 \text{ s}^{-1}$ of the Cs $39d$ state [23] is close to the calculated blackbody photoionization, but the ionization rates of the Cs $40p$ and Rb $40s$ states are not.

In summary, the measurements reported here demonstrate clearly that excitation to an attractive, as opposed to a repulsive potential dramatically increases the initial ionization rate due to dipole-dipole induced collisions. However, atoms excited to repulsive curves also ionize at rates in excess of the expected blackbody ionization rates. We suggest that in this case the attractive atom-atom or ion-atom potentials lead to increased ionization. The complete dynamics of the ionization of an ensemble of Rydberg atoms is complex, but the attractive dipole-dipole or dipole-ion forces are the main parameter for this problematic.

The authors acknowledge fruitful discussions with Vladimir Akulin. This work is in the frame of "Institut Francilien de Recherche sur les Atomes Froids" (IFRAF)

-
- [1] I. Mourachko *et al.*, Phys. Rev. Lett. **80**, 253 (1998).
[2] W. R. Anderson *et al.*, Phys. Rev. Lett. **80**, 249 (1998).
[3] A. Fioretti *et al.*, Phys. Rev. Lett. **82**, 1839 (1999).
[4] D. Jaksch *et al.*, Phys. Rev. Lett. **85**, 2208 (2000).
[5] M. D. Lukin *et al.*, Phys. Rev. Lett. **87**, 037901 (2001).
[6] D. Tong *et al.*, Phys. Rev. Lett. **93**, 063001 (2004).
[7] T. Vogt *et al.*, Phys. Rev. Lett. **99**, 073002 (2007).
[8] J. S. Frasier *et al.*, Phys. Rev. A **59**, 4358 (1999).
[9] W. M. Akulin *et al.*, Physica D **131**, 125 (1999).
[10] T. Vogt *et al.*, Phys. Rev. Lett. **97**, 083003 (2006).
[11] M. P. Robinson *et al.*, Phys. Rev. Lett. **85**, 4466 (2000).
[12] T. C. Killian *et al.*, Phys. Rev. Lett. **83**, 4776 (1999).
[13] T. C. Killian, T. Pattard, T. Pohl, and J. M. Rost, Phys. Report **449**, 77 (2007).
[14] A. Walz-Flannigan *et al.*, Phys. Rev. A **69**, 063405 (2004).
[15] T. Amthor *et al.*, Phys. Rev. Lett. **98**, 023004 (2007).
[16] J. O. Day, E. Brekke, and T. G. Walker, Phys. Rev. A **77**, 052712 (2008).
[17] A. Reinhard, T. Cubel Liebisch, K. C. Younge, P. R. Berman, and G. Raithel, Physical Review Letters **100**, 123007 (2008).
[18] W. Li *et al.*, Phys. Rev. A **70**, 042713 (2004).
[19] P. J. Tanner, J. Han, E. S. Shuman, and T. F. Gallagher, Phys. Rev. Lett. **100**, 043002 (2008).
[20] W. Li *et al.*, Phys. Rev. Lett. **94**, 173001 (2005).
[21] I. I. Beterov, D. B. Tretyakov, I. I. Ryabtsev, A. Ekers, and N. N. Bezuglov, Phys. Rev. A **75**, 052720 (2007).
[22] T. Wang, S. F. Yelin, R. Côté, E. E. Eyler, S. M. Farooqi, P. L. Gould, M. Koštrun, D. Tong, and D. Vrinceanu, Phys. Rev. A **75**, 033802 (2007).
[23] B. Laburthe-Tolra, PhD thesis, Université Paris Sud XI (2001).
[24] The ionization time is simply calculated by integrating the dipole-dipole forces between two Rydberg atoms:

$$U(R) = \frac{W_{pp-ss'}}{2} \left(1 + \sqrt{1 + \left(\frac{\mu\mu'}{R^3 W_{pp-ss'}/2} \right)^2} \right)$$